Polymerization Catalysts with d^n Electrons ($n = 1-4$): A Theoretical Study

Rochus Schmid‡ and Tom Ziegler*

Department of Chemistry, University of Calgary, 2500 University Drive NW, Calgary, Canada T2N 1N4

Received September 21, 1999

We present an investigation on the potential of first-row transition metals with a d-electron count from 1 to 4 as olefin polymerization catalysts by means of first-principles density functional theory (DFT) type calculations. We considered generic model systems $[MLL'R]^+$ with M = Ti, V, Cr, and Mn (R = Me, Et) in high-spin electron configuration bearing two nitrogen ligands L,L′ (NH_2^- and NH_3) in order to elucidate the effect of partially filled d-levels on the elementary steps of ethylene polymerization. The olefin uptake energy is found to diminish almost linearly with an increasing number of d-electrons due to a successive destabilization of the metal acceptor orbital. Ethylene insertion barriers were calculated to be between 6 and 16 kcal/mol (R = Et) and are less affected by the d-electron count than by the type of the transition metal and its oxidation state. The dominant termination process for most systems is a β-hydrogen transfer (BHT) to the monomer. Its barrier follows the trends of the olefin insertion, but is higher in absolute values for the majority of systems. In the case of the Cr(IV) d^2 system, with the overall best performance, possible real size catalysts were investigated. It is shown that by taking the specific electronic situation in d^n systems into account, olefin insertion barriers below 10 kcal/mol together with high termination barriers can be achieved.

Introduction

The range of homogeneous polymerization catalysts has grown steadily since the discovery of active group IV metallocene systems by Kaminsky in 1976.[1] A systematic modification of the substituents on the ligand framework of *ansa*-bridged metallocene catalysts (**1**) led to significant improvements in both activity and selectivity toward isotactic and syndiotactic polymerization of propylene.[2] The so-called "constrained geometry" catalysts (**2**) with *ansa*-bridged cyclopentadienyl (Cp) amide ligands demonstrated that a bis-Cp framework is not a necessary prerequisite for catalytic activity.[3] McConville et al. found a living polymerization system with a sterically demanding diamide ligand (**3**).[4] Meanwhile, a wide variety of active polymerization catalysts with group III/IV transition metals, lanthanides, and actinides stabilized with a broad range of auxiliary ligands have emerged.[5] These developments were accompanied by a large number of theoretical investigations on the principal reaction mechanism as well as specific ligand effects.[6] In a recent series of papers, a unified view of ethylene polymerization catalysis by d^0 and d^0f^n metals was presented based on density functional theory (DFT) type calculations.[7]

Apart from these polymerization catalysts with a d^0 electron configuration, a number of late transition metal polymerization systems were discovered recently. It was shown by Brookhart et al. that Ni(II) and Pd(II) complexes (**4**) with a d^8 electron count can be modified from olefin oligomerization catalysts to active polymerization catalysts by increasing the steric bulk of the auxiliary ligands.[8] This effect originates from a larger

‡ Present address: Technische Universität München, Anorganisch-Chemisches Institut, D-85747 Garching, Germany.

(1) Andersen, A. A.; Cordes, H. G.; Herwig, J.; Kaminsky, W.; Merck, A.; Mottweiler, R.; Pein, J.; Sinn, H.; Vollmer, H. J. *Angew. Chem., Int. Ed. Engl.* **1976**, *15*, 630.

(2) (a) Spalek, W.; Antberg, M.; Rohrmann, J.; Winter, A.; Bachmann, B.; Kiprof, P.; Behm, J.; Herrmann, W. A. *Angew. Chem., Int. Ed. Engl.* **1992**, *31*, 1347. (b) Brinzinger, H. H.; Fischer, D.; Mühlhaupt, R.; Rieger, B.; Waymouth, R. M. *Angew. Chem., Int. Ed. Engl.* **1995**, *34*, 1708.

(3) (a) Canich, J. A. M. Eur. Pat. Appl., EP 420436, 1990. (b) Stevens, J. C.; Neithammer, D. R. Eur. Pat. Applic., EP 418044, 1990. (c) Stevens, J. C.; Timmers, F. J.; Wilson, D. R.; Schmidt, G. F.; Nicklas, P. N.; Rosen, R. K.; Knight, G. W.; Lai, S. Y. Eur. Pat. Appl., EP 416815, 1990. (d) Canich, J. A. M. US Pat. Appl., 5,026,798 and 5,055,438, 1993.

(4) (a) Scollard, J. D.; McConville, D. H. *J. Am. Chem. Soc.* **1996**, *118*, 10008. (b) Scollard, J. D.; McConville, D. H.; Payne, N. C.; Vittal, J. J. *Macromolecules* **1996**, *29*, 5241. (c) Guérin, F.; McConville, D. H., Vittal, J. J. *Organometallics* **1996**, *15*, 5586. (d) Scollard, J. D.; McConville, D. H.; Rettig, S. J. *Organometallics* **1997**, *16*, 1810. (e) Scollard, J. D.; McConville, D. H.; Vittal, J. J. *Organometallics* **1997**, *16*, 4415. (f) Scollard, J. D.; McConville, D. H.; Vittal, J. J. *Organometallics* **1997**, *16*, 4415. (g) Gibson, V. C.; Kimberley, B. S.; White, A. J. P.; Williams, D. J.; Howard, P. *J. Chem. Soc., Chem. Commun.* **1998**, 313.

(5) Bochmann, M. *J. Chem. Soc., Dalton Trans.* **1996**, 255.

(6) (a) Jolly, C. A.; Marynick, D. S. *J. Am. Chem. Soc.* **1989**, *111*, 7968. (b) Castonguay, L. A.; Rappé, A. K. *J. Am. Chem. Soc.* **1992**, *114*, 5832. (c) Kawamura-Kuribayashi, H.; Koga, N.; Morokuma, K. *J. Am. Chem. Soc.* **1992**, *114*, 2359. (d) Kawamura-Kuribayashi, H.; Koga, N.; Morokuma, K. *J. Am. Chem. Soc.* **1992**, *114*, 8687. (e) Weiss, H.; Ehrig, C.; Ahlrichs, R. *J. Am. Chem. Soc.* **1994**, *116*, 4919. (f) Woo, T. K.; Fan, L.; Ziegler, T. *Organometallics* **1994**, *13*, 2252. (g) Woo, T. K.; Fan, L.; Ziegler, T. *Organometallics* **1994**, *13*, 432. (h) Yoshida, T.; Koga, N.; Morokuma, K. *Organometallics* **1995**, *14*, 746. (i) Lohrenz, J. C. W.; Woo, T. K.; Ziegler, T. *J. Am. Chem. Soc.* **1995**, *117*, 12793. (j) Woo, T.; Margl, P. M.; Lohrenz, J. C. W.; Blöchl, P. E.; Ziegler, T. *J. Am. Chem. Soc.* **1996**, *118*, 13021.

(7) (a) Margl, P. M.; Deng, L.; Ziegler, T. *Organometallics* **1998**, *17*, 933. (b) Margl, P. M.; Deng, L.; Ziegler, T. *J. Am. Chem. Soc.* **1998**, *120*, 5517. (c) Margl, P. M.; Deng, L.; Ziegler, T. *J. Am. Chem. Soc.* **1999**, *121*, 154.

10.1021/om9907425 CCC: $19.00
Publication on Web 06/13/2000

Scheme 1. Polymerization Catalysts

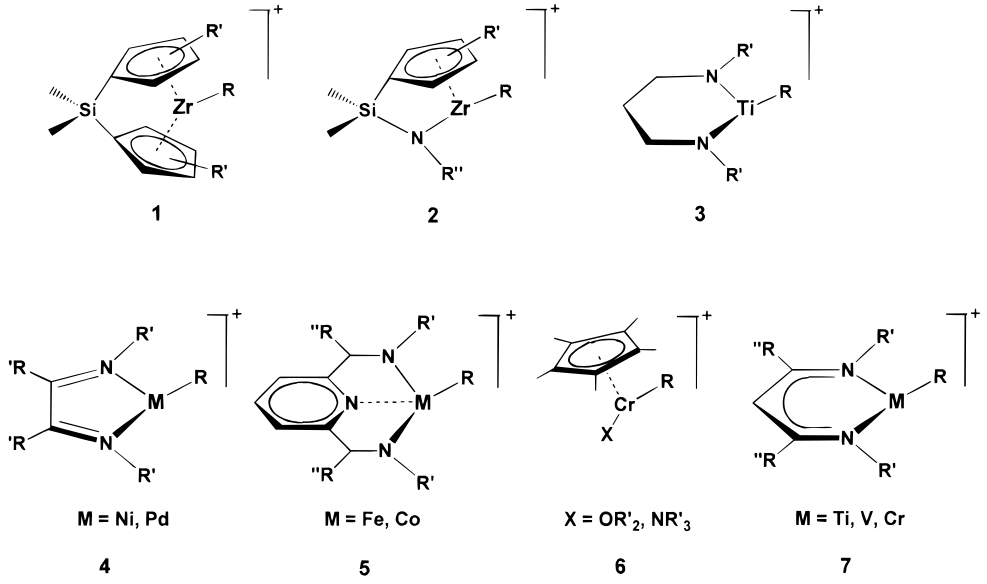

1 **2** **3** **4** **5** **6** **7**

destabilization of the chain termination transition state relative to the chain propagation transition state by steric strain, as it has been verified by theoretical calculations.[9] Very recently, Brookhart et al. and Gibson et al. have shown that this concept can also be extended to Fe(II) and Co(II) complexes (**5**) with d^6 and d^7 electron configurations, respectively.[10] To model the silica-supported active sites of the heterogeneous Union-Carbide[11] and Phillips[12] polymerization catalyst, a number of groups have investigated corresponding Cr(III) model systems. A Cr(III) complex of type **6** with $X = OR_2$ was found to polymerize ethylene,[13] and a similar *ansa*-bridged system with $X = NR_3$ was shown to have quite remarkable activities.[14] The feasibility of direct ethylene insertion into the M−C bond for such d^3 Cr(III) systems has been investigated theoretically by Jensen and Børve[15] on the model of $[CrCl(H_2O)CH_3]^+$. Very recently, Theopold et al. reported that M(III) complexes (M = Ti, Cr, V) with the so-called "nacnac" ligand (substituted β-diiminate) (**7**) catalyze the homopolymerization of ethylene as well as the copolymerization of ethylene with α-olefins.[16]

Scheme 2. Model Systems

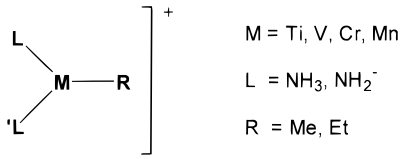

These promising experimental results for metal centers with one or more d-electrons raise the general question under which conditions systems with a d-electron count between zero and eight may act as active polymerization catalysts. This is equivalent to answering the question of *how occupied d-orbitals influence the elementary steps involved in olefin polymerization*. It is the aim of an ongoing project in our group to investigate this problem by means of theoretical calculations. Here, we present our first results on model systems of first-row transition metals with a d-electron count from 1 to 4 as depicted in Scheme 2.

To be able to differentiate between steric and electronic effects, we restricted ourselves in the first instance to cationic model systems with a set of two nitrogen ligands, a coordination environment found in a number of the above-mentioned systems (**3**, **4**, **7**). The ligands being either amine (NH_3) or amide (NH_2^-) give rise to oxidation states of the metal atom of II to IV, which leads to d-electron populations between 1 and 4 for different metal ligand combinations. Because similar 3d systems are known from experiment[16,17] to be in a high-spin state, we shall restrict our discussion to systems in a high-spin electronic configuration.[18] We have chosen at least two different systems for each d-electron count, which are reasonable in terms of experimental knowledge.[17] As shown in Scheme 2, an alkyl substituent R (R = Me, Et) represents the growing polymer chain. Table 1 lists all systems that have been considered in this investigation according to their precursor complexes. To facilitate the discussion, we

(8) (a) Johnson, L. K.; Killian, C. M.; Brookhart, M. *J. Am. Chem. Soc.* **1995**, *117*, 6414. (b) Johnson, L. K.; Mecking, S.; Brookart, M. *J. Am. Chem. Soc.* **1996**, *118*, 267. (c) Killian, C. M.; Tempel, D. J.; Johnson, L. K.; Brookhart, M. *J. Am. Chem. Soc.* **1996**, *118*, 11664. (d) Rix, F. C.; Brookhart, M.; White, P. S. *J. Am. Chem. Soc.* **1996**, *118*, 4746.

(9) (a) Deng, L.; Margl, P. M.; Ziegler, T. *J. Am. Chem. Soc.* **1997**, *119*, 1094. (b) Deng, L.; Woo, T. K.; Cavallo, L.; Margl, P. M.; Ziegler, T. *J. Am. Chem. Soc.* **1997**, *119*, 6177. (c) Froese, R. D. J.; Musaev, D. G.; Morokuma, K. *J. Am. Chem. Soc.* **1998**, *120*, 1581. (d) Musaev, D. G.; Froese, R. D. J.; Morokuma, K. *Organometallics* **1998**, *17*, 1850.

(10) (a) Brookhart, M.; DeSimone, J. M.; Tanner, M. J. *Macromolecules* **1995**, *28*, 5378. (b) Tanner, M. J.; Brookhart, M.; DeSimone, J. M. *J. Am. Chem. Soc.* **1997**, *119*, 7617. (c) Small, B. L.; Brookhart, M.; A., B. A. M. *J. Am. Chem. Soc.* **1998**, *120*, 4049. (d) Britovsek, G. J. P.; Gibson, V. C.; Kimberley, B. S.; Maddox, P. J.; McTavish, S. J.; Solan, G. A.; White, A. J. P.; Williams, D. J. *Chem. Commun.* **1998**, 849.

(11) Karol, F. J.; Karapinka, G. L.; Wu, C.; Dow, A. W.; Johnson, R. N. Carrick, W. L. *J. Polym. Sci., Part A-1* **1972**, *10*, 2621.

(12) Hogan, J. P. *J. Polym. Sci., Part A-1* **1970**, *8*, 2637.

(13) (a) Thomas, B. J.; Noh, S. K.; Schulte, G. K.; Sendlinger, S. C.; Theopold, K. H. *J. Am. Chem. Soc.* **1991**, *113*, 893. (b) Bhandari, G.; Kim, Y.; McFarland, J. M.; Rheingold, A. L.; Theopold, K. H. *Organometallics* **1995**, *14*, 738. (c) White, P. A.; Calabrese, J.; Theopold, K. H. *Organometallics* **1996**, *15*, 5473.

(14) Emrich R.; Heinemann, O.; Jolly, P. W.; Krüger, C.; Verhovnik, G. P. J. *Organometallics* **1997**, *16*, 1551.

(15) Jensen, V. R.; Børve, K. J. *Organometallics* **1997**, *16*, 2514.

(16) (a) Kim, W.-K.; Fevola, M. J.; Liable-Sands, L. M.; Rheingold, A. L.; Theopold, K. H. *Organometallics* **1998**, *17*, 4541. (b) Budzelaar, P. H. M.; van Oort, A. B.; Orpen, A. G. *Eur. J. Inorg. Chem.* **1998**, 1485.

Table 1. Precursor Complexes (R = Me, Et) and Corresponding Nomenclature for All Systems Investigated in This Study

	Ti	V	Cr	Mn
d^1	$[Ti(NH_2)(NH_3)R]^+$ **Ti1**	$[V(NH_2)_2R]^+$ **V1**		
d^2		$[V(NH_2)(NH_3)R]^+$ **V2**	$[Cr(NH_2)_2R]^+$ **Cr2**	
d^3		$[V(NH_3)_2R]^+$ **V3**	$[Cr(NH_2)(NH_3)R]^+$ **Cr3**	$[Mn(NH_2)_2R]^+$ **Mn3**
d^4			$[Cr(NH_3)_2R]^+$ **Cr4**	$[Mn(NH_2)(NH_3)R]^+$ **Mn4**

abbreviate the systems by the metal and the d-electron occupation, which uniquely defines also the oxidation state and the type of ligands. To differentiate between the systems with R = Et and R = Me, the latter will be referenced by the system label plus Me (e.g., **Ti1Me**).

It should be noted that the calculations on these three-coordinate cationic model systems are only an initial but necessary step in the search for active polymerization catalysts with d-electrons. They are unbiased from steric effects and allow for a direct comparison with each other and also the model systems of the experimentally more established d^0 catalysts. Thus they can serve as a tool in order to understand the underlying electronic effects of occupied d-levels and provide a lead for more advanced systems. In the last section of this work we focus on one promising system, which was studied with realistic types of ligands including steric effects.

Computational Details

All calculations were performed with the density functional theory (DFT) program package ADF, developed by Baerends et al.,[19] using the numerical integration scheme developed by te Velde et al.[20] The frozen core approximation was employed throughout. For the transition metal atoms (Ti, V, Cr, Mn), a triple-ζ Slater type basis set for the 3s, 3p, 3d, and 4s valence shells plus one 4p polarization function, and for silicon a triple-ζ STO basis set for the 3s and 3p valence shell plus one 3d polarization function, was used. Nonmetal atoms were described by a double-ζ STO basis with one 3d (C, N) or one 2p (H) polarization function.[21] A set of auxiliary s, p, d, f, and g STO functions, centered on all nuclei, was used in order to fit the molecular density and present Coulomb and exchange potentials accurately in each SCF cycle.[22] For all calculations, the local exchange−correlation potential by Vosko et al.[23] was augmented with gradient-corrected functionals for electron exchange according to Becke[24] and correlation according to Perdew[25] in a self-consistent fashion. This nonlocal density functional is usually termed BP86 in the literature and has proven to be reliable for both geometries and energetics of transition metal systems. Metal−ligand dissociation energetics obtained on this level of theory were shown to be correct to within 5 kcal/mol of the experimental result and were usually overestimated in absolute terms.[26,27] Activation energies are generally calculated to be 2−4 kcal/mol lower than the experimental estimate.[26,27] In a recent benchmark computational study, Jensen and Børve have shown that the BP86 functional gives results in excellent agreement with the best wave function-based methods available today, for the class of reactions investigated here.[28] All calculations were performed in a spin-unrestricted fashion. First-order scalar relativistic corrections[29] were added to the total energy for all systems, since a perturbative relativistic approach is sufficient for first-row transition metals as shown by Deng et al.[30] No symmetry constraints were applied. Activation energies were determined by minimizing all degrees of freedom while keeping a specific internal coordinate, representing the reaction coordinate, fixed. This procedure of locating the stationary point by minimizing the force along the reaction coordinate (threshold of 0.0015 au) gives only an upper bound for the activation energy. However, from our considerable experience in the calculation of insertion and termination transition states of the similar d^0 and d^8 systems[7] we know that this procedure gives results converged within a fraction of a kcal/mol compared to those from transition state search algorithms, and it is therefore sufficiently accurate for the problem at hand. Due to the number of systems investigated and the computational effort connected with the calculation of the second derivatives of the energy with respect to the nuclei positions, we refrained from zero-point energy and finite-temperature corrections. A discussion of these effects on the example of a Zr-d^0 catalyst can be found in ref 6i.

Results and Discussion

Elementary Steps of Olefin Polymerization. As already known from studies on d^0 and d^8 polymerization catalysts, three reaction steps have to be investigated in order to judge the catalytic properties of a particular metal system (Scheme 3). The first step of the chain propagation is the binding of ethylene to the precursor which forms the olefin complex (**OC**). We will refer to the energy difference between the precursor and the olefin complex as "uptake" energy. Because of the

(17) (a) Alyea, E. C.; Bradley, D. C.; Lappert, M. F.; Sanger, A. R. *Chem. Commun.* **1969**, 1064. (b) Alyea, E. C.; Bradley, D. C. *J. Chem. Soc. (A)* **1969**, 2330. (c) Minhas, R. K.; Edema, J. J. H.; Gambarotta, S.; Meetsam, A. *J. Am. Chem. Soc.* **1993**, *115*, 6710. (d) Berno, P.; Gambarotta, S.; Kotila, S.; Erker, G. *J. Chem. Soc., Chem. Commun.* **1996**, 779. (e) Jezierski, A.; Raynor, J. B. *J. Chem. Soc., Dalton Trans.* **1981**, 1. (f) Basi, J. S.; Bradley, D. C.; Chisholm, M. H. *J. Chem. Soc. (A)* **1971**, 1433. (g) Danopulos, A. A.; Wilkinson, G.; Sweet, T. K. N.; Hursthouse, M. B. *J. Chem. Soc., Dalton Trans.* **1995**, 2111. (h) Hao, S.; Song, J.-I.; Berno, P.; Gambarotta, S. *Organometallics* **1994**, *13*, 1326. (i) Howard, C. G.; Girolami, G. S.; Wilkinson, G.; Thornton-Pett, M.; Hursthouse, M. B. *J. Chem. Soc., Chem. Commun.* **1983**, 1163. (j) Choukroun, R.; Moumboko, P.; Chevalier, S.; Etienne, M.; Donnadieu, B. *Angew. Chem., Int. Ed. Engl.* **1998**, *37*, 3169.
(18) Test calculations on a number of our model systems showed in all cases that high-spin was the preferred ground-state configuration.
(19) (a) Baerends, E. J.; Ellis, D. E.; Ros, P. *Chem. Phys.* **1973**, *2*, 41. (b) Baerends, E. J.; Ros, P. *Chem. Phys.* **1973**, *2*, 52.
(20) te Velde, G.; Baerends, E. J. *J. Comput. Chem.* **1992**, *99*, 84.
(21) Snijders, J. G.; Baerends, E. J.; Vernoijs, P. *At. Nucl. Data Tables* **1982**, *26*, 483.
(22) Krijn, J.; Baerends, E. J. *Fit Functions in the HFS Method*; Department of Theoretical Chemistry, Free University: Amsterdam, The Netherlands, 1984.
(23) Vosko, S. H.; Wilk, L.; Nusair, M. *Can. J. Phys.* **1980**, *58*, 1200.
(24) Becke, A. *Phys. Rev. A* **1988**, *38*, 3098.
(25) (a) Perdew, J. P. *Phys. Rev. B* **1986**, *34*, 7406. (b) Perdew, J. P. *Phys. Rev. B* **1986**, *33*, 8822−8824.
(26) Margl, P.; Ziegler, T. *Organometallics* **1996**, *15*, 5519.
(27) Margl, P. M.; Ziegler, T. *J. Am. Chem. Soc.* **1996**, *118*, 7337.
(28) Jensen, V.; Borve, K. *J. Comput. Chem.* **1998**, *19*, 947.
(29) (a) Snijders, J. G.; Baerends, E. J. *Mol. Phys.* **1978**, *36*, 1789. (b) Snijders, J. G.; Baerends, H. J.; Ros, P. *Mol. Phys.* **1979**, *38*, 1909.
(30) Deng, L.; Ziegler, T.; Woo, T.; Margl, P.; Fan, L. *Organometallics* **1998**, *17*, 3240.

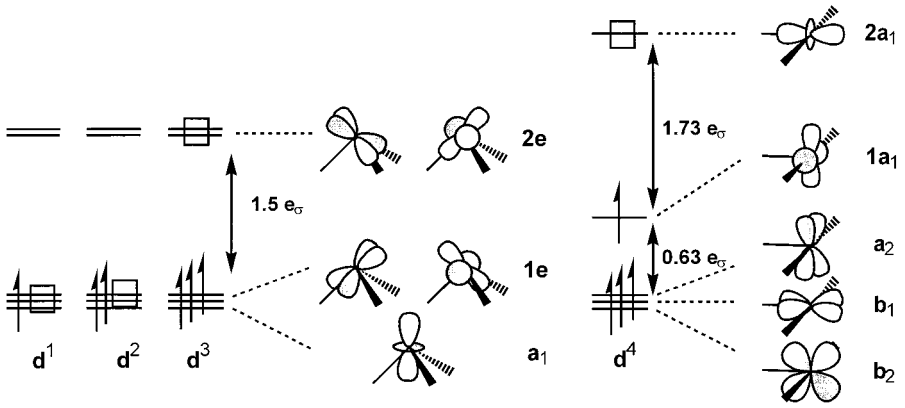

Figure 1. Frontier d-orbitals of the $[M(L)(L')R]^+$ fragment for d^1 to d^4 high-spin systems in a trigonal pyramidal (pseudo-C_{3v} symmetry; left) and T-shaped geometry (pseudo-C_{2v} symmetry, right). The open square denominates the empty acceptor orbital for the π-d donation from the olefin.

Scheme 3. Elementary Steps of Chain Propagation and Chain Termination

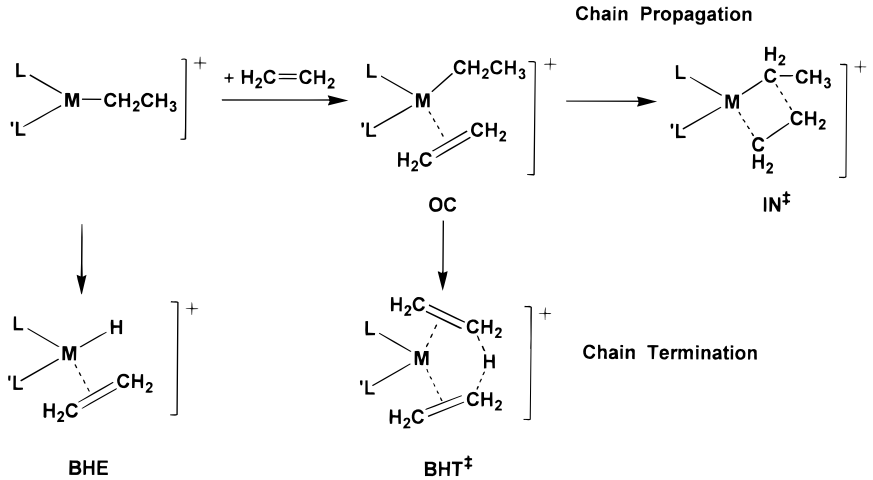

intrinsic entropic penalty of the bimolecular olefin uptake reaction, a high binding energy of ethylene and a low insertion barrier are necessary for reasonable catalytic activity. The next and crucial elementary reaction is the olefin insertion into the metal carbon bond, which proceeds via the insertion (**IN**) transition state. The energy difference between **IN** and **OC** is the insertion barrier. To achieve high molecular weight polymer (polymerization instead of oligomerization), the insertion barrier must be well below all possible termination barriers. As shown in Scheme 3, termination reactions to be considered are the β-hydrogen elimination (**BHE**) leading from the precursor to the corresponding hydrido olefin complex and the β-hydrogen transfer reaction (**BHT**) which starts from the **OC**. The **BHT** termination barrier is given by the energy difference between the **BHT** transition state and the **OC**. The **BHE** termination barrier will be higher than the energy difference between the precursor and the **BHE** product, which we refer to as **BHE** reaction energy. We calculated the **BHE** transition state only for those systems where the **BHT** termination barrier was significantly higher than the thermodynamic barrier of the **BHE** reaction.

Ethylene Binding. The bonding mechanism of ethylene to the $[M(L)(L')(R)]^+$ precursor consists of π-d donation from the olefin into the empty d-orbitals and, in the case of filled d-levels, the d-π* back-donation. In contrast to d^0 systems, the presence of filled d-orbitals has a directing effect on all metal ligand interactions. Figure 1 displays in schematic form[31] the metal d-orbitals for the three-coordinate $[M(L)(L')(R)]^+$ precursor (under the assumption of three equivalent ligands and only σ-type interactions). This represents the frontier orbitals of the metal fragment interacting with the incoming olefin. Up to a d-electron count of 3, a C_{3v}-symmetric pyramidal geometry is preferred (Figure 1 left). For a d^4 system, however, a C_{2v}-symmetric T-shaped geometry is formed (Figure 1 right), because in a pyramidal structure a very destabilized 2e orbital would have to be occupied.

The acceptor orbital for the olefin-to-metal π-d donation (denoted by an empty square in Figure 1) for both d^1 and d^2 systems is the empty d_{z^2} orbital (a_1), since the unpaired electrons can occupy one or both of the degenerate 1e orbitals. This results in a tetrahedral olefin complex similar to d^0 systems (Figure 2). In the d^3 configuration, however, the third unpaired electron will occupy this a_1 acceptor orbital, and the olefin can interact with only one of the high lying empty 2e orbitals. The lobes of this acceptor orbital are not located on the C_3-axis of the metal fragment, which leads to a distortion from a tetrahedral geometry in d^3 olefin complexes as shown schematically in Figure 2. For a T-shaped d^4 precursor, the olefin interacts with the most

(31) Albright, T. A.; Burdett, J. K.; Whangbo, M. H. *Orbital Interactions in Chemistry*; John Wiley & Sons: New York, 1984.

Table 2. Calculated Reaction Energies for the Model Systems

			R = Me			R = Et			
	L,L′		E_{uptake} [kcal/mol]	$E_{insertion}$ [kcal/mol]		E_{uptake} [kcal/mol]	$E_{insertion}$ [kcal/mol]	$E_{\beta H-transfer}$ [kcal/mol]	$E_{\beta H-elimination}$ [kcal/mol]
Ti1	$(NH_2)(NH_3)$	d^1	−31.4	17.4	BS	−27.7	14.2	18.5	13.6
					FS	−26.8	14.3		
V1	$(NH_2)_2$	d^1	−29.4	12.4	BS	−21.4	9.5	14.1	15.3
					FS	−24.6	11.1		
V2	$(NH_2)(NH_3)$	d^2	−24.9	11.8	BS	−22.9	14.4	12.4	13.2
					FS	−23.1	13.0		
Cr2	$(NH2)_2$	d^2	−24.5	8.2	BS	−18.4	6.3	13.2	16.2
					FS	−20.1	9.3		
V3	$(NH_3)_2$	d^3	−15.7	10.8		−14.4	11.5	11.1	15.4
Cr3	$(NH_2)(NH_3)$	d^3	−15.1	15.0		−13.5	15.6	21.2	21.1
Mn3	$(NH_2)_2$	d^3	−15.6	12.3		−13.7	11.1	15.0	23.7
Cr4	$(NH_3)_2$	d^4	−13.6	12.6		−12.1	11.1	17.5	18.4
Mn4	$(NH_2)(NH_3)$	d^4	−11.5	11.5		−11.1	10.8	16.9	22.9

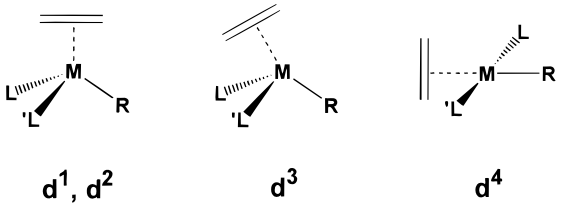

Figure 2. Schematic representation of the **OC** geometries.

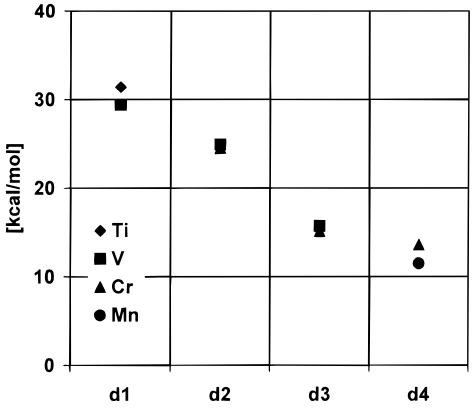

Figure 3. Uptake energies of the R = Me systems.

destabilized empty $2a_1$ orbital (as indicated by the empty square in Figure 1 on the right), resulting in a square-planar geometry of the corresponding olefin complex (Figure 2). This is similar to the orbital-directing effects leading to square-planar geometries of d^8 complexes, which have four doubly occupied d-levels.

All calculated **OC** structures exhibit the discussed features shown in Figure 2. The inequivalence of the three ligands L, L′, and R, and π-interactions of both the olefin and the amide ligands with metal d-orbitals, however, lead to certain structural deviations (the amide metal π-interaction in the **Cr2** system is discussed in the last section of this paper). To save page space, we refrain here from a detailed analysis of the calculated geometries.[32]

The structure of **OC** for the ethyl systems shows the same trends as discussed above. Because of the β-agostic interaction, which formally acts as a fifth ligand, the geometries are slightly more distorted than the complexes with R = Me. The d^1 and d^2 **OC** allow for two different structures. We use the nomenclature of "front side" (**FS**) and "backside" (**BS**) complex, as it was introduced for the tetrahedral d^0 systems.[6i,j] The difference between these coordination modes can be viewed as the olefin being either trans (**BS**) or cis (**FS**) with respect to the β-agostic hydrogen in a pseudo-trigonal bipyramidal geometry (Scheme 4). For the nontetrahedral d^3 and d^4 systems this classification is no longer valid. We found only one preferred **OC** geometry for the d^3 systems.

In Table 2 the calculated olefin uptake energies for all systems (R = Me and Et) are given. The binding energies of complexes with different metal ligand combinations but similar d-electron count are nearly identical, as shown in Figure 3 for R = Me. In contrast to that, the uptake energy decreases significantly when the number of d-electrons is increased. This tendency can

Scheme 4. Backside and Frontside Olefin Complex

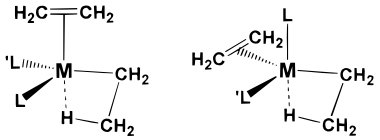

be understood in terms of the same orbital interactions, which were discussed before in order to explain the **OC** geometries. It is obvious from the orbital diagram given in Figure 1 that sequential filling of the d-orbitals with 1−4 electrons leads to a more and more destabilized acceptor orbital for the olefin π-d donation, which diminishes the binding energy. The contribution from the d-π* back-donation, on the other hand, is almost constant, because only one singly occupied d-orbital with the proper symmetry is available, irrespective of the number of d-electrons. This simplified picture explains the large drop of the uptake energy between d^2 and d^3 and also the lowest values for d^4 systems, but it fails to explain the difference between d^1 and d^2. The latter effect is due to the fact that one of the two orbitals labeled as 1e in Figure 1 (left) is destabilized from a π-interaction with an amide ligand present for all d^1 and d^2 systems (a detailed analysis of this kind of interaction is given in the last section). This does not affect the d^1 systems, but in the case of d^2 systems, this destabilized orbital must be occupied in the **OC**, which reduces the ethylene binding energy.

The olefin uptake energies for the corresponding ethyl complexes follow the same general trends, but they are

(32) A complete listing of the calculated Cartesian coordinates of all stationary points is given in the Supporting Information.

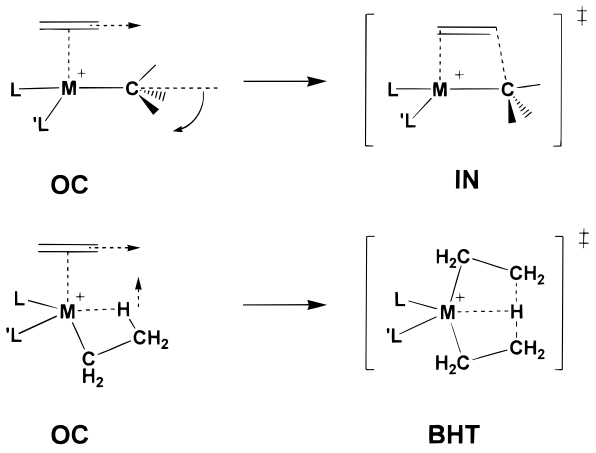

Figure 4. Reaction coordinate of the olefin insertion and the β-hydrogen transfer reaction (**BHT**).

slightly smaller in absolute terms due to the higher steric strain. The dependence of the uptake energy on the accessible surface of the metal atom has already been observed for d^0 catalysts;[7a] the differences here are nevertheless modest.

Chain Propagation. The essential step of the chain propagation is the insertion of the olefin into the metal−carbon bond. The reaction coordinate for this process, leading from the **OC** to the insertion transition state (**IN**, see Scheme 3), involves a η^2 to η^1 shift of the π-bonded olefin toward the alkyl group and a rotation of the alkyl group in the insertion plane (Figure 4). For certain systems an additional rotation of the ethylene fragment into the insertion plane is necessary. At the transition state, one carbon atom of the olefin and the alkyl sp^3 carbon atom approach each other to form the new C−C bond.

Figure 5 shows a simplified orbital interaction diagram for this process in the case of a d^1 electron configuration (neglecting all perturbations from the auxiliary ligands). The two highest doubly occupied orbitals of the **OC** on the left side are the metal−olefin π-bond (π-d donation) and the metal−alkyl σ-bond. These are both mainly ligand-centered orbitals well below the metal d-levels. By mixing with the π*-orbital of the olefin, one d-orbital of proper symmetry (π* b.) is significantly stabilized and is therefore occupied by an unpaired electron. This interaction represents the d-π* back-donation discussed in the previous section.

At the transition state (**IN**) the former metal−alkyl and metal−olefin bonding orbitals mix with each other. Additionally, they get polarized (and thereby energetically stabilized) by the π*-orbital of the olefin, which is no longer accessible for d-π* back-donation. As a result, the new M−C and C−C bond to be formed remain roughly on the same energy level as the original ligand-centered orbitals (sp^3 and π b.). In contrast to this, the stabilizing interaction of one of the d-orbitals (d-π* back-donation) is lost at **IN** and the unpaired electron now occupies an energetically higher lying orbital of metal d-character. This destabilization of exactly one unpaired electron is the major contribution to the electronic barrier of the olefin insertion for the high-spin d^1 to d^4 systems.

In Table 2, the olefin insertion barriers for all systems investigated are summarized. The insertion barriers for

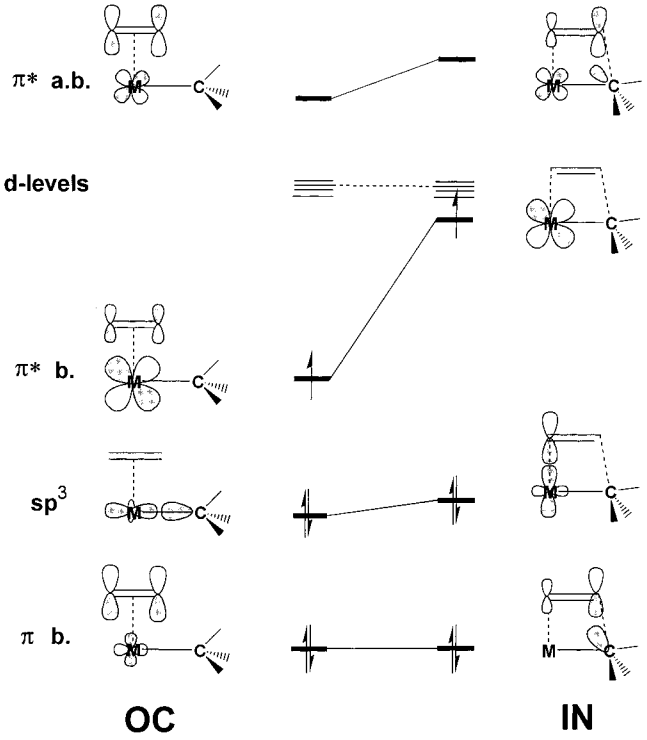

Figure 5. Simplified orbital interaction diagram for the olefin insertion reaction.

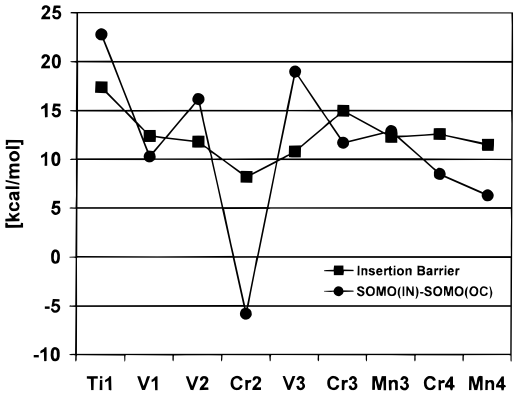

Figure 6. Olefin insertion barrier and the destabilization of the lowest SOMO when going from **OC** to **IN** (R = Me).

the R = Me range from the highest value of 17.4 kcal/mol for **Ti1Me** down to 8.2 kcal/mol for **Cr2Me**. It is obvious that the variations for different d occupations are much smaller than those for the olefin uptake energy. Only one d-orbital is destabilized in the **IN** transition state irrespective of the total number of unpaired d-electrons. Therefore, the barrier is mainly determined by the strength of this d-π* back-donation for different metal−ligand combinations; more diffuse or higher lying d-orbitals induce a higher insertion barrier. For the corresponding d^0 model system [Ti(NH$_2$)$_2$R]$^+$ no d-π* back-donation is present, which leads to a comparably low insertion barrier of only 5 kcal/mol (BS).[7b] Figure 6 correlates the insertion barriers of the methyl systems with the difference of the Kohn−Sham orbital energies of the lowest singly occupied orbital of the **IN** and **OC** (SOMO(**IN**) − SOMO(**OC**)). One has to keep in mind that the correlation in Figure 6 focuses only on one orbital, but for a first-principles method like DFT, the total energy is not the sum of the orbital

energies. Therefore it is astonishing how well this orbital destabilization reflects the overall tendencies of the insertion barriers. Interestingly, **Cr2Me** having the lowest insertion barrier with only 8.2 kcal/mol is the only system where this lowest SOMO is actually more stabilized at the transition state **IN** compared to the **OC**.

Both the d^1 and d^2 systems are structurally very similar to generic d^0 catalysts including the **BS** and **FS** insertion mode for the corresponding ethyl complexes. However, the insertion barriers are significantly higher because of the d-π* back-donation, and the overall trend is matched by the destabilization of the lowest SOMO (Figure 5). The strength of the d-π* back-donation decreases with decreasing d-orbital energies. Consequently, the insertion barrier decreases when going from left to right in the periodic table for a given d-occupation (e.g., **Ti1Me** → **V1Me**). On the basis of the same argument, we would also expect a significant increase of the insertion barrier when going from 3d to 4d and 5d transition metals.

The trend of the insertion barriers for the d^3 systems deviates much more from SOMO destabilization than for the d^1 and d^2 catalysts, and the tendency of decreasing barriers by going to the right in the periodic table is no longer seen. It should be noted that all the molecular orbitals involved in the insertion process (Figure 5) are energetically influenced by the d-electron occupation. The geometries of the **OC** of the d^3 complexes (Figure 2) vary quite significantly for different ligand environments. Especially for **Cr3Me**, a strong deformation can be observed when the system moves on the insertion reaction coordinate from the **OC** to **IN**. At 15.0 kcal/mol, this system has the highest insertion barrier after **Ti1Me**.

The d^4 catalysts show low insertion barriers, reflected by small SOMO destabilizations. The square-planar **OC** of **Cr4Me** has two isomers with the NH_3 ligands either cis or trans to each other, with the trans arrangement being more stable ($\Delta E_{cis/trans}$ = 3.5 kcal/mol). The reaction coordinate of both isomers leads however to the same **IN** transition state with a cis coordination of the auxiliary ligands. It resembles structurally the insertion transition states found for the square-planar d^8 catalysts (**4**).[9] However, because of the single occupation of the d-orbitals, the insertion barriers (**Cr4**, 11.1; **Mn4**, 10.8 kcal/mol) are nearly twice as low as the corresponding sterically uncongested Ni-d^8 systems (**4b** with R′ = H: 17.5 kcal/mol[9]). Due to the interaction of the amide lone pair with the empty d-orbital in **Mn4Me**, the **OC** is not square planar. This interaction also prevents a cis coordination of the N-ligands and gives rise to a distorted square-planar geometry even in the **IN** transition state.[32]

The insertion barriers for complexes with R = Et follow the general trend for those with R = Me (Table 2). The absolute values are slightly lower than for R = Me, due to the destabilization of the **OC** by steric strain, as already observed for the olefin uptake reaction. This strain is diminished in the course of the insertion reaction, which lowers the barrier.

Chain Termination Reactions. From the theoretical studies on both d^0 and d^8 systems,[7c,9,33] it is known that only the β-hydrogen transfer reaction (**BHT**) and the β-hydrogen elimination (**BHE**) must be considered as chain termination mechanisms (Scheme 3). The calculations generally afforded higher barriers for **BHE** compared to **BHT**. To verify this, we calculated the thermodynamic endothermicity of the **BHE** reaction in addition to the kinetic termination barrier for **BHT.** Table 2 lists the energy differences between **OC** and **BHT** transition state ($E_{H-transfer}$) and between the precursor and the hydrido olefin product of the **BHE** process ($E_{\beta-elim}$). In accordance with our previous work on d^0 catalysts, the **BHT** barrier for the tetrahedral d^1 and d^2 systems is given with respect to the **FS** olefin complex.[7c]

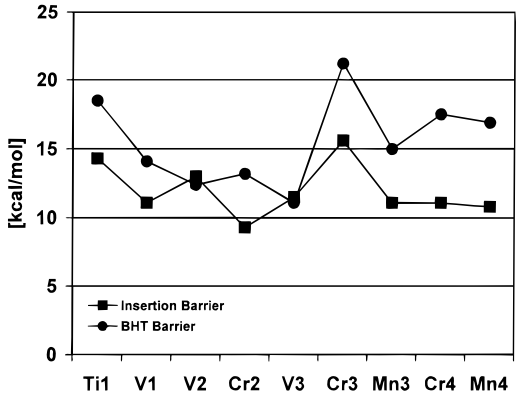

Figure 7. Insertion barriers and **BHT** termination barriers (R = Et).

The **BHE** reaction is very endothermic for all systems considered, with the thermodynamic barrier already higher than the kinetic **BHT** barrier (with the exception of **Ti1)**. One driving force for this reaction is the formation of d-π* back-donation in the hydrido olefin complex. However, for the systems considered here, this interaction is weak, which leads to the low insertion barriers, but also makes the **BHE** reaction unfavorable. **Ti1** shows both the highest insertion barrier and the lowest thermodynamic **BHE** barrier, due to its diffuse and high lying d-orbitals. Because of the **BHE** reaction energy of **Ti1** (13.6 kcal/mol) being much lower than the **BHT** barrier (18.5 kcal/mol), we also calculated the **BHE** transition state, which affords an effective termination barrier of 14.5 kcal/mol via **BHE**.

As depicted in Figure 4, the transition state of the **BHT** reaction is pseudo-C_s-symmetric, with the transferred hydrogen atom being midway between the two β-carbon atoms. The energy profile at the transition state is very sharp, and the major contribution to the energy barrier arises from breaking the C−H bond. In analogy to the insertion process, this is associated with a shift of the olefin out of the optimal π-bonding coordination mode. Therefore, the tendencies observed for the **BHT** termination barriers reflect those of the insertion barriers, as shown graphically in Figure 7. With the exception of **V2** and **V3** the termination barriers are above the insertion barriers by about 3−5 kcal/mol because of the high and roughly constant activation energy necessary to break the C−H bond.

It should be noted that a termination barrier higher than the corresponding barrier of chain propagation is

(33) Woo, T. K.; Margl, P.; Ziegler, T.; Blöchl, P. E. *Organometallics* **1997**, *16*, 3454.

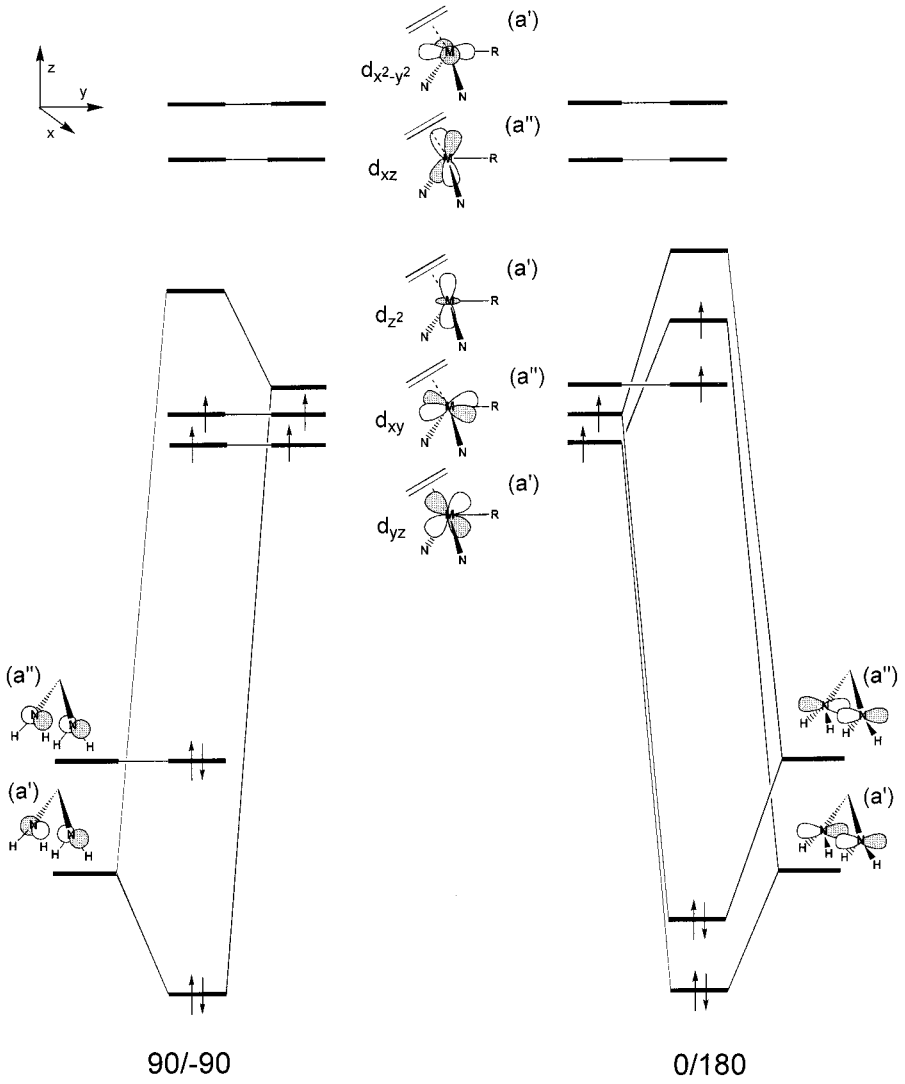

Figure 8. Metal−ligand orbital interactions in the **OC** of **Cr2**.

a necessary prerequisite for active polymerization catalysts. For the bis-amide Ti d^0 catalysts (**3**) and the Ni/Pd d^8 catalysts (**4**), the generic systems exhibit a lower termination than insertion barrier.[4,8,9,30] This can be reversed only by the inclusion of steric strain exerted by the auxiliary ligands. In contrast to that, for the d^1 to d^4 catalysts investigated here, already the generic systems have a termination barrier generally above the insertion barrier. Therefore, all systems should be considered as potential polymerization catalysts. For a given d-electron count, a high oxidation state should be preferred, because this leads to a contraction of the d-orbitals and therefore to lower insertion barriers.

A Possible Cr(IV) d^2 Polymerization Catalyst. From an overall point of view the **V1**, **Cr2**, and **Mn3** systems with an oxidation state of IV are of special interest, with **Cr2** being the most promising. In this section we present the results of our initial efforts to design a real size ligand for a possible Cr(IV) polymerization catalyst. To achieve a realistic Cr(IV) catalyst, the two amide ligands present in the model system of **Cr2** have to be converted into a realistic ligand system with both electronic and steric effects taken into account. A number of bidentate amide ligands stabilizing M(IV) complexes are known, e.g., those employed in the Ti(IV)-based system (**3**).[4] However, for a high-spin d^2

Scheme 5. Possible Arrangements of the Two Amide Ligands

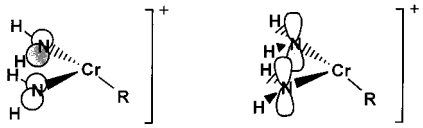

system, important additional electronic effects have to be considered. These are due to the interaction of the two lone pairs of the amide ligands with the metal d-orbitals. Two extreme arrangements of the amides with the p-type lone pairs either in the N−M−N plane (90/−90) or perpendicular to it (0/180) are possible, as shown in Scheme 5 (the nomenclature refers to the H−N−M−N dihedral angle). These two conformations lead to significant differences in the nature of the two singly occupied orbitals, which has important consequences for the catalytic properties of the system.

The origin of this difference is displayed in Figure 8. Due to the strong metal−ligand interactions involved in the covalent M−N and M−C bonds, the $d_{x^2-y^2}$ and d_{xz} orbitals are destabilized the most. The weaker π-d donation from the olefin brings the d_{z^2} orbital above the two lowest lying orbitals of d_{yz} and d_{xy} character. For the 90/−90 arrangement the latter two orbitals of d_{xy}

Table 3. Calculated Reaction Energies for $[Cr(L)(R)]^+$ Systems with R = Et (All Energies Are Given in kcal/mol and Are Based on the BS OC)

	ligand	constraint	E_{uptake}	$E_{insertion}$	$E_{termination}$[a]
Cr2	$(NH_2)_2$		−18.4	6.3	11.5
Cr2	$(NH_2)_2$	90/−90	−17.5	5.2	10.6
Cr2	$(NH_2)_2$	0/180	−15.9	11.3	12.4
Cr2-A	$(NMe_2)_2$		−14.7	11.9	18.6
Cr2-B	$(N(SiH_3)_2)_2$		−10.4	9.4	20.2
Cr2-C	$NH(CH_2)_3NH$		−16.8	13.2	14.8
Cr2-D	$N((CH_2)_4)_2N$		−9.3	8.4	22.6

[a] **BHT** termination reaction.

and d_{yz} character remain the lowest and are both singly occupied, since only the symmetric (a′) combination of the amide lone pairs interacts with the d_{z^2} orbital and destabilizes the latter. The antisymmetric combination (a″) can only interact with the d_{xz} orbital, which is energetically too high. In contrast to that, for the 0/180 arrangement of the amides both a′ and a″ are able to interact with exactly these two orbitals (d_{xy} and d_{yz}). As a consequence, the d_{z^2} orbital is now the SOMO. Both because of a weaker interaction with the a′ amide lone pair combination and the d-π* back-donation interaction, the d_{yz} orbital holds the second unpaired electron.

The olefin insertion process takes place in the plane of symmetry and affects only orbitals of a′ symmetry. Because of the new M−C bond formed in the transition state and the loss of d-π* back-donation, both d_{z^2} and d_{yz} are destabilized in the transition state, which makes the olefin insertion less favorable for the 0/180 arrangement than for 90/−90. In Table 3 the reaction energies for olefin uptake, insertion, and BHT termination are given for **Cr2** constrained to either a 90/−90 or a 0/180 arrangement of the amide ligands. Because of the unavailability of the d_{xy} orbital, the 0/180 system possesses an insertion barrier about twice as high as the 90/−90 conformation. This is reflected in the sum of the orbital energies of the SOMOs, when going from the **OC** to the **IN** transition state: for 90/−90 they are destabilized by 0.23 eV compared to 0.54 eV for the 0/180 conformation.

It should be noted that the energy levels in Figure 8, although qualitative, correctly represent the ordering of the calculated Kohn−Sham orbitals for these systems. Figure 9 shows the two SOMOs for a symmetry-enforced **OC** with R = Me.[34] The absolute orbital energies are additionally affected by the fact that for the 0/180 arrangement the donation from the amides to the metal is larger and the two SOMOs are of higher energy, compared to the 90/−90 conformation. This increases the strength of the d-π* back-donation to the olefin and therefore the olefin insertion barrier. This leads us to the conclusion that a 90/−90 conformation is optimal for a d^2 polymerization catalyst.

To move toward more realistic systems, we have chosen the ligand systems that are shown in Scheme 6 in the form of the corresponding Cr(IV) alkyl cations. For all these systems we calculated the elementary reactions of olefin uptake, insertion, and **BHT** termination (Table 3). As expected, the olefin uptake energies are not affected by the specific conformation of the ligand system. However, they decline with an increasing size of the auxiliary ligand due to an increasing steric destabilization of the **OC**.

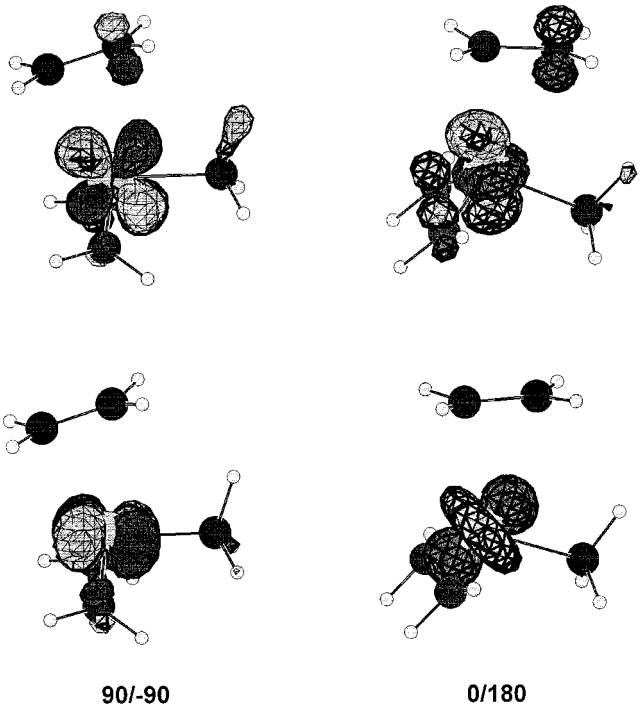

Figure 9. Singly occupied KS orbitals of the **OC** of **Cr2Me** (enforced C_s symmetry).[34]

Scheme 6. Cationic Precursors of Realistic Cr(IV) Systems Investigated

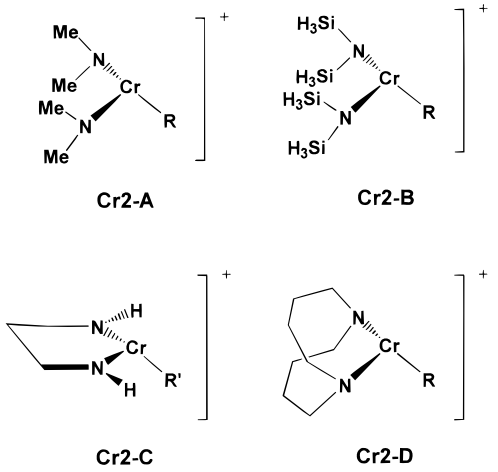

Cr2-A and **Cr2-B** represent the strategy of a straightforward substitution of the simple amides with alkyl or silyl groups, forming a complex with two nonchelating ligands. Due to electronic and steric reasons, these ligands maintain the preferred 90/−90 coordination mode throughout all reactions. Only the precursor complex of **Cr2-B** shows a geometry with one ligand in a 90/−90 mode and the other close to 0/180 due to an agostic interaction of one of the silyl hydrogen atoms with the metal center.[35] Both insertion and termination barriers are increased with respect to the model system

(34) The analysis of the KS orbitals calculated by ADF has been performed with the program *viewkel* (part of the YAeHMOP program package by Greg Landrum available at http://ionic.chem.cornell.edu/landrum/yaehmop.html).

(35) Herrmann, W. A.; Eppinger, J.; Spiegler, M.; Runte, O.; Anwander, R. *Organometallics* **1997**, *16*, 1813.

Cr2, because of the steric and electronic differences that arise from the substitution of the hydrogen with a CH_3 or SiH_3 group, respectively. However, because of the 90/−90 arrangement, the energetic separation between **IN** and **BHT** transition states (6.7 and 10.8 kcal/mol, respectively) is even larger than for the generic system (5.2 kcal/mol). We are aware of the fact that the missing chelating effect for these systems might allow for unfavorable side reactions during catalyst synthesis and activation. However, in particular **Cr2-B** must be seen as a potential catalyst, with an insertion barrier of only 9.4 kcal/mol, and an outstandingly high termination barrier of 20.2 kcal/mol. It should be noted that homoleptic alkyl (NEt_2) and silyl amides ($N(SiMe_3)_2$) are experimentally accessible and often serve as a starting point in Cr(IV) chemistry.[14]

In the case of the chelating ligand system in **Cr2-C,** the backbone forces the amides into a 0/180 conformation. This is preferential for d^0 systems[7b] but turns the **Cr2-C** system into a poor catalyst: as expected, **Cr2-C** shows an overall reaction energy profile very similar to the model system constrained to 0/180. The insertion barrier is as high as 13.2 kcal/mol, and especially the energetic separation between the insertion and termination barrier has gone down from 5.2 kcal/mol for **Cr2** to 1.6 kcal/mol for **Cr2-C**. The unfavorable energetics for **Cr2-C** is a result of its 0/180 conformation (Figure 8). The insertion barrier of **Cr2-C**, however, still compares with other systems and does not prevent catalytic activity in general. It is known for the equivalent Ti(IV) catalysts (**3**) that the inclusion of steric bulk on the nitrogen atoms increases the energetic separation of **IN** and **BHT** transition states.[30] Therefore, **Cr2-C** might still be converted into an active catalytic system, but the advantageous electronic situation of the **Cr2** model system is lost.

To prevent this, **Cr2-D** represents our suggestion for a system that maintains both the advantages of a chelating ligand structure and a 90/−90 arrangement of the amides. On the basis of preliminary calculations, we concluded that at least a four-membered chain is necessary for the two links between nitrogen to allow for a strain-free coordination of the ligand to the metal atom. With only 8.4 kcal/mol, **Cr2-D** has the lowest insertion barrier of all substituted systems. The **BHT**-termination barrier of 22.6 kcal/mol is even higher than for **Cr2-B**, which leads to a large energetic separation between insertion and termination of 14.2 kcal/mol. We want to point out that the simple alkyl backbone should be seen as a first attempt to maintain the amide conformation in **Cr2-A** in a chelating ligand structure. More advanced systems with a lower steric demand can be envisioned, because of the unique situation that for the Cr(IV) d^2 catalysts, a large energetic separation between the insertion and termination transition states can already be achieved without steric strain of the auxiliary ligands. In an upcoming study we investigate in a similar manner the experimentally known real size systems of type **7** with M = Ti, V, Cr. In addition we suggest new variations from these systems, designed on the basis of the results gained in this work.[36]

Conclusion

Our calculations on generic model systems of the type $[ML_2R]^+$ with two simple nitrogen ligands (L = NH_2^-, NH_3) demonstrate that all high-spin first-row transition metal complexes with up to four d-electrons must be considered as potential olefin polymerization catalysts. The olefin uptake energy declines with an increasing number of d-electrons, because of an increasingly destabilized acceptor orbital. The olefin insertion barriers are low, with values down to only 6.3 kcal/mol for **Cr2**. The dominant termination mechanism is the **BHT** reaction**,** with barriers generally about 3 kcal/mol above the olefin insertion barrier. Systems with a high oxidation state and a d-electron count up to three (**V1**, **Cr2**, **Mn3**) have the best overall catalytic potential. These findings reveal the basic electronic effects of populated d-orbitals on the elementary steps, which might however be altered by steric encumbrance and changes of the coordination number as well as solvent and counterion interactions.[37] To derive real size Cr(IV) complexes of **Cr2**, specific electronic interactions with the two auxiliary amide ligands have to be considered. With ligand systems that allow a perpendicular arrangement of the amide planes with respect to the N−Cr−N plane (90/−90), low insertion barriers below 10 kcal/mol and a very high insertion/termination separation could be achieved. Readily available Cr(IV) complexes with nonchelating bis-alkyl or bis-silyl amides can be employed, but also more complex chelating structures with a double link between the nitrogen atoms are very promising.

Acknowledgment. This investigation has been generously supported by Novacor Research and Technology Corporation (NRTC) of Calgary, and the National Sciences and Engineering Research Council (NSERC) of Canada. We also wish to thank Peter Margl and Liqun Deng for helpful discussions and suggestions in this project.

Supporting Information Available: A listing of the total energies and the Cartesian coordinates of all calculated species is available. This material is available free of charge via the Internet at http://pubs.acs.org.

OM9907425

(36) Schmid, R.; Deng, L.; Ziegler, T. Submitted for publication.
(37) Chan, M. S. W.; Vanka, K.; Pye, C. C.; Ziegler, T. *Organometallics* **1999**, *18*, 4624.